CrystEngComm

PAPER

View Article Online
View Journal | View Issue

Cite this: *CrystEngComm*, 2017, **19**, 5122

One-step exfoliation of ultra-smooth β-Ga_2O_3 wafers from bulk crystal for photodetectors

Wenxiang Mu,[a] Zhitai Jia, *[ac] Yanru Yin,[a] Qiangqiang Hu,[a] Jian Zhang,[a] Qian Feng,[b] Yue Hao[b] and Xutang Tao *[a]

Received 9th June 2017,
Accepted 1st August 2017

DOI: 10.1039/c7ce01076a

rsc.li/crystengcomm

High-quality bulk β-Ga_2O_3 single crystals have been grown by optimized edge-defined film-fed growth (EFG) method. The problems of cracking and polycrystals have been effectively solved by using a high-quality 1 inch-wide seed. The crystalline quality of the as-grown crystal has been confirmed by X-ray rocking curve with a full-width at half-maximum (FWHM) of 42.1 arcsec. Moreover, an economical and efficient one-step mechanical exfoliation method has been proposed to get epi-ready β-Ga_2O_3 wafers directly. The root mean square (RMS) roughness of the wafers is noted to be around 0.1 nm, which means they are comparable or even better than wafers processed by chemical mechanical polishing (CMP). The mechanism of the exfoliation method is analyzed from a crystallographic view. A photodetector is fabricated on the exfoliated wafer directly and the device is proved to show good performance in solar-blind band.

Introduction

In recent years, much attention has been paid to wide-bandgap semiconductors for their broad range of applications in industry and science.[1–3] For example, GaN-based light emitting diodes (LEDs) with advantages of high efficiency, low energy consumption and long lifetime are widely used as environmentally friendly light sources.[4] However, optoelectronic devices operating at short wavelengths and high-voltage power devices are still not mature.[1,5] As we all know, the increase in bandgap benefits the performance in a short-wavelength emission and breakdowns electric field. Besides, the development of wide-bandgap materials opens new application fields of such semiconductors in short-wavelength LEDs, laser diodes (LDs) and photodetectors, as well as high-voltage power devices supported by high breakdown field.[6] The demand for ultraviolet optoelectronic devices and high-voltage power devices encourages the growth and characterization of new materials with wider bandgaps.

The band gap of β-Ga_2O_3 is as wide as ~4.8 eV, which is much larger than that of traditional 4H-SiC (3.2 eV), GaN (3.4 eV)[7] and ZnO (3.4 eV).[8] In addition, β-Ga_2O_3 single crystal can be grown from melt, just like silicon and sapphire. The access to large-sized bulk crystals makes the fabrication of optoelectronic devices and electronic devices realizable. Therefore, β-Ga_2O_3 has recently attracted considerable attention and is expected to be a next-generation semiconductor material due to its promising functions for high-voltage power devices[9–12] and ultraviolet optoelectronic devices.[13–15] Solar irradiation between 190 and 280 nm cannot reach the surface of the Earth because of the absorption of stratospheric ozone. Solar-blind photodetectors can detect very weak signals due to little background disturbance. Thus, solar-blind photodetectors have attracted a lot of attention due to numerous potential applications in the fields of fire detection and intersatellite communication as well as biological and environmental fields.[14] β-Ga_2O_3 is a direct semiconductor with an ultraviolet cutoff edge of about 260 nm, which is located in the solar-blind spectra band. So, it is an ideal material for fabricating solar-blind photodetectors, in particular, photodetectors can be fabricated based on β-Ga_2O_3 without alloying, which is required in the cases of GaN and ZnO. Besides, some other applications in power devices, high-temperature gas sensors[16] and substrates for GaN-based high-brightness LEDs[17] have also been reported. Overall, the excellent physical properties and device performances of β-Ga_2O_3 stimulate the growth of high-quality bulk single crystals.

β-Ga_2O_3 has a monoclinic structure ($C2/m$)[18] with lattice constants of a = 12.23 Å, b = 3.04 Å, c = 5.08 Å, and β = 103.8°. It is a congruently melting compound with a melting point of 1740 °C.[19] Therefore, β-Ga_2O_3 can be grown by melt-growth methods such as Verneuil process,[20] optical floating-zone

[a] *State Key Laboratory of Crystal Materials & Key Laboratory of Functional Crystal Materials and Device, Shandong University, Jinan, 250100, China. E-mail: z.jia@sdu.edu.cn, txt@sdu.edu.cn*
[b] *State Key Discipline Laboratory of Wide Band Gap Semiconductor Technology, School of Microelectronics, Xidian University, Xi'an 710071, China*
[c] *State Key Laboratory of Optoelectronic Materials and Technologies, Sun Yat-sen University, Guangzhou 510275, China*

method,[21] Czochralski process,[22,23] edge-defined film-fed growth (EFG) method,[24–26] and Bridgman technique.[27] Lately, large-sized bulk crystals have been grown *via* the EFG method.[24] In this reported crystal growth process, the neck cross-section should be shrunk to very small size in order to get a single crystal without polycrystalline inclusions.[24] However, this necking process is very difficult to be controlled and the occurrence of polycrystalline inclusions during shouldering is still a major challenge that hinders the growth of high-quality, large-sized β-Ga_2O_3 single crystal by the EFG method.

In semiconductor industry, bulk crystals have to be cut and polished to smooth wafers for device fabrication or to be used as substrates for film epitaxies. Substrate is crucial for semiconductor industry,[28] even a slight lattice mismatch between the substrate and epitaxial layer has an obvious impact on crystal quality. Therefore, native substrate is desired and only highly crystalline wafer with smooth and flat surface can be used as the substrate for epitaxial growth.[1] However, β-Ga_2O_3 crystal is difficult to be cut and polished due to its cleavage nature. Therefore, it is a big challenge to obtain high-quality wafers from bulk crystals through traditional processing methods. On the other hand, exfoliation has been adopted in getting two-dimensional materials such as graphene, MoS_2, and BN.[29,30] Meanwhile, large-sized crystal plates can also be exfoliated through mechanical or chemical methods. For instance, Kim *et al.* exfoliated the epitaxial layer from GaAs substrate with the help of graphene,[28] while Mahenderkar *et al.* exfoliated 2 inch single-crystal Au foils with the help of chemical etching.[31] β-Ga_2O_3 wafer can also be exfoliated from the bulk crystal owing to its strong cleavage nature, similar to two-dimensional materials.

In the first part of this work, we design a unique Ir die, lid and after-heater accounting for Ga_2O_3 decomposition together with Ir oxidization at high temperature. Afterwards, high-quality β-Ga_2O_3 single crystal with 25 mm width and 98 mm length is successfully grown by using a high-quality 1 inch-wide seed to avoid cracking and the formation of polycrystalline morphology. In the second part, a simple one-step method is proposed to achieve high surface quality (100) wafers by a direct mechanical exfoliation process. To evaluate wafer quality for the crystal's application in device fabrication, surface quality of the obtained wafers is examined in detail, and then a solar-blind photodetector is fabricated directly on the exfoliated (100) wafer.

Experimental section

Crystal growth

β-Ga_2O_3 single crystals were grown by the EFG method using an RF induction furnace. β-Ga_2O_3 powders (purity 99.99%) were pressed into tablets, which were subsequently loaded into an iridium crucible of Φ 60 × 60 mm^3 in dimensions with an Ir lid on top of the crucible. The top surface of the Ir die was several millimeters higher than the Ir lid. Seven capillaries with a diameter of 0.3 mm or a slit with a width of 0.3 mm ran through the whole Ir die. The size of the die top was 4 × 25 mm^2 with a flat surface. An Ir after-heater (Φ 60 × 100 mm^3) was used to reduce thermal stress in the crystal. We heated the melt to a temperature slightly higher than the melting point of β-Ga_2O_3 for two or three hours to release gas in the melt. When all materials were melted, the melt was transported from the crucible to the die top through the capillaries or the slit by capillary action. The seed was dipped onto the surface of the die slowly and repeatedly until a suitable temperature was reached at which seed diameter became constant. Different seed sizes and growth parameters were used in our experiment. For conventional seeds of about 5 mm width, we started pulling the seed at 15 mm h^{-1} and adjusted heating power to neck the seed, then gradually reducing the pulling speed to 5–7 mm h^{-1} and, at the same time, decreasing the temperature to let the crystal spread across the whole top of the die. In the case of 1 inch-wide seeds, the seed was pulled at 5–7 mm h^{-1} at a suitable temperature and necking and shouldering were avoided. Crystal growth was carried out in a mixed gas atmosphere containing 70% CO_2, 1% O_2 and 29% N_2. The CO_2 in the atmosphere decomposed into O_2 and CO at high temperature. Therefore, the mixed gas atmosphere protected the iridium crucible and obtained relatively high oxygen partial pressure to reduce decomposition and evaporation of Ga_2O_3 at high temperature.

Characterization techniques

High-resolution X-ray diffraction (HRXRD) was conducted using Bruker D8 Discovery system equipped with a four-crystal monochromator set for Cu Kα_1 radiation (λ = 1.54056 Å). The voltage and current of the generator were 40 kV and 40 mA, respectively. The step time and step size were 0.4 s and 0.001°, respectively. A (100) facing exfoliated wafer was used as the HRXRD sample with dimensions of about 7 × 7 × 0.5 mm^3. Room-temperature optical transmission spectra of exfoliated (100) facing wafer were measured using a Lambda 900 double-beam UV/vis/IR spectrometer in the UV-vis-near-IR range and with a Nicolet NEXUS 670 FTIR spectrometer in the mid-IR region. The surface topography of the exfoliated wafers was recorded by an atomic force microscope (AFM) with Agilent 5500 in tapping mode and the scanning range was 5 × 5 μm^2 with a scan speed of 5.9982 $\mu m\ s^{-1}$. The top surface topography of the Ir die was observed by Leica DM2700 M optical microscope.

Result and discussion

Growth of the β-Ga_2O_3 crystal and characterization

In our experiments, we found that crystals always tended to become polycrystals during shouldering due to the cleavage habit of β-Ga_2O_3, as shown in Fig. 1a. Other researchers were also bothered by this problem.[24] In order to solve it, we used a 1 inch-wide seed to avoid shouldering. The 1 inch-wide seed was obtained by cutting the crystal (Fig. 1a) perpendicular to the grown direction. The wide seed was melted back 0.5–1 mm to eliminate defects on the surface induced by

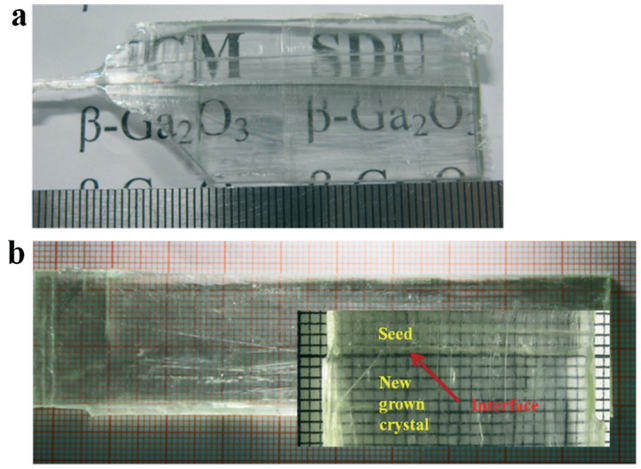

Fig. 1 Crystals grown with small size seed (a) and 1 inch-wide seed (b) by the EFG method.

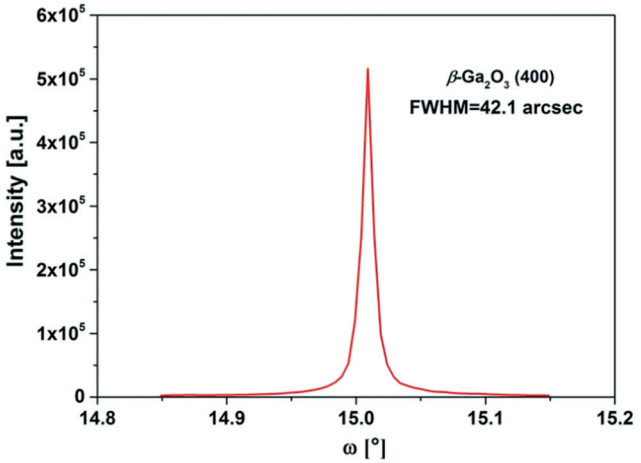

Fig. 3 Rocking curve of the β-Ga_2O_3 crystal wafer.

cutting. It was found that high-quality single crystals without polycrystalline inclusions can be easily grown using a wide seed, as shown in Fig. 1b.

β-Ga_2O_3 has a monoclinic structure and two cleavage planes of (100) and (001). Therefore, polycrystalline inclusions or twin crystals are likely to occur for β-Ga_2O_3. In addition, the top surface of the Ir die is very rough on the micro level, as shown in Fig. 2. The microcosmic defects of the die would form a new crystal nucleus. Therefore, crystal shouldering on the die surface is relatively difficult. Polycrystalline inclusions and cracking tend to be induced during shouldering process due to the formation of a new crystal nucleus.

The crystalline quality of the as-grown crystal was checked by HRXRD. The full-width at half-maximum (FWHM) of the rocking curve was 42.1″ (Fig. 3), which was comparable to that of the crystal sample grown by the CZ[23] and EFG methods.[24]

The UV-vis-NIR and mid-IR transmittance of β-Ga_2O_3 crystal is shown in Fig. 4. β-Ga_2O_3 exhibited a very broad transmission range from 0.26 to 7.33 μm. The bandgap of β-Ga_2O_3 was estimated to be 4.73 eV by the standard fitting, as shown in the inset of Fig. 4a. The drop in transmittance in the infrared band was caused by free-carrier absorption.[23]

β-Ga_2O_3 wafer

β-Ga_2O_3 has two cleavage planes, (100) and (001). Among them, cleavage along the (100) plane is easier. (100) facing wafers were exfoliated by a thin sharp knife from the bulk crystal; the exfoliation process is shown in Fig. 5. In order to get large-sized and high-quality wafers, high-quality crystal samples with different annealing processes were exfoliated. The samples with dimensions of about 7 × 7 × 3 mm^3 were annealed in Ar or O_2 atmosphere for 30 hours at 1100 °C and then cooled down to room temperature at a rate of 20–30 °C h^{-1}. For comparison, the samples used in the exfoliation experiment were cut from the same as-grown crystal.

In our experiment, small (100) facing wafers with a side length about 3 mm can be obtained from the crystal samples without annealing. The wafers tend to break up when the side length exceeds 3 mm. However, large-sized (100) facing wafers are more difficult to be exfoliated from the crystal samples after annealing in O_2 atmosphere, because these wafers tend to break into crystal flakes or needles, as shown in Fig. 6a. In contrast, large-sized (100) facing wafers can be easily exfoliated from the crystal samples after annealing in Ar atmosphere, as shown in Fig. 6b. The reason for the exfoliation can be explained by the structure of the crystal. The

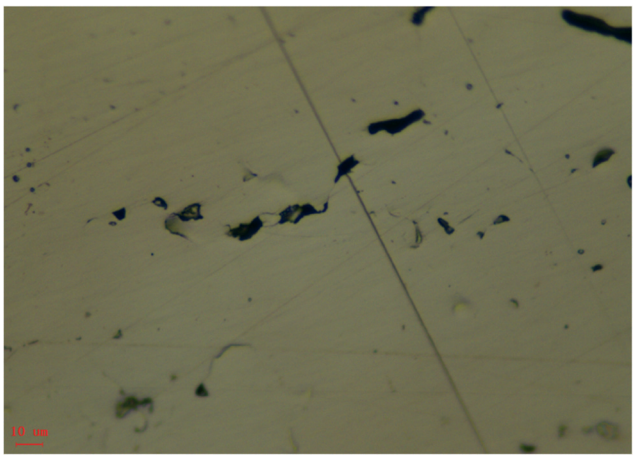

Fig. 2 Top surface of the Ir die under optical microscope.

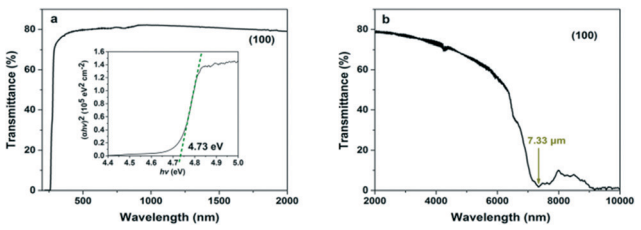

Fig. 4 (a) UV-vis-NIR (b) mid-IR transmission spectra of the β-Ga_2O_3 crystal.

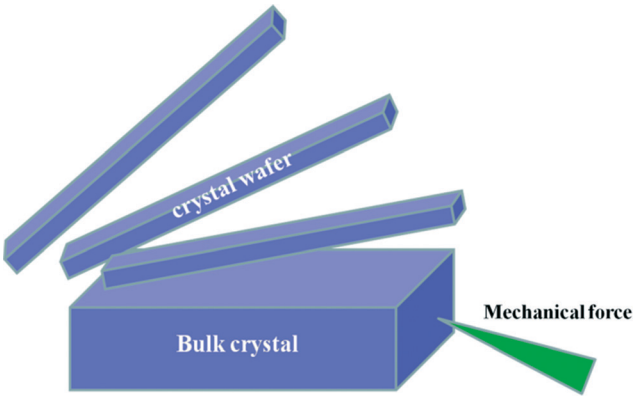

Fig. 5 Schematic representation of exfoliation.

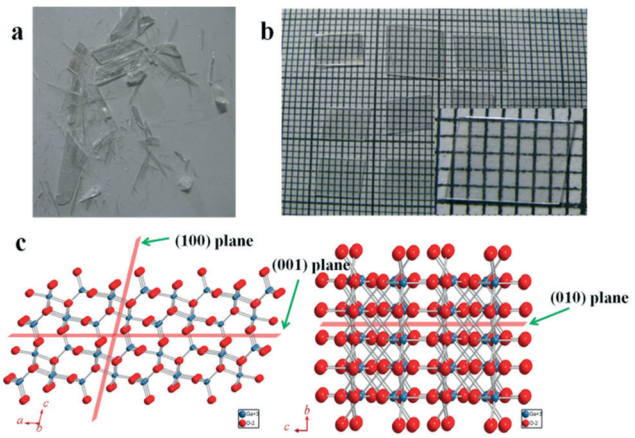

Fig. 6 (a) Cracked flakes exfoliated from as-grown crystal before annealing (b) wafers fabrication by mechanical exfoliation after annealing in Ar atmosphere. (c) Ball-and-stick diagram of β-Ga_2O_3.

crystal structure of β-Ga_2O_3 is shown in Fig. 6c. As we can see, the space distributions of the chemical bonds along the three crystal axes are different. The bonds between the (010) plane forms a three-dimensional network, which can effectively resist outer shear fore. There are three-dimensional network bonds and parallel bonds between the (001) plane. In contrast, the bonds between the (100) plane are parallel to each other. Therefore, the (100) plane is the easiest one to be broken down under external shear force.

The effect of different annealing processes on mechanical exfoliation may be due to the change in concentration of oxygen vacancies and reduction in stress on the crystal. Ar atmosphere annealing increases the concentration of oxygen vacancies and reduces stress on the annealed crystal simples. High concentration of oxygen vacancies is beneficial for separation of adjacent planes and reducing stress that decreases the break probability in mechanical exfoliation. The concentration of oxygen vacancies is reduced after O_2 atmosphere annealing and greater force is required in the exfoliation process. The wafers can break up on the (001) plane under large force in the mechanical exfoliation process. Therefore, it is difficult to get a large-sized wafer. The as-grown crystal has a moderate concentration of oxygen vacancies but stress on the crystal is very large and it increases break probability. Therefore, large-sized crystal wafers are easily obtained from the crystal after annealing in Ar atmosphere.

High surface quality of wafers is essential in semiconductor technology, and usually, wafers should be processed by chemical mechanical polishing (CMP) technique to reduce the roughness. The benefit of β-Ga_2O_3 is that high surface quality wafers can be obtained directly by mechanical stripping without the complicated CMP process. In this work, root mean square (RMS) surface roughness values of the as-obtained wafers are in the range of 0.043 to 0.1 nm, as shown in Fig. 7, which means that the substrate surface was good enough to be directly used for epitaxy or device fabrication. This exfoliation method is a one-step low-cost technique compared to traditional machining processes. Moreover, there is no damaged layer on the exfoliated wafer surface in theory, benefiting from no requirement of cutting and grinding in the exfoliation method. This is beneficial for film epitaxy and device fabrication.

Solar-blind photodetector

To check the feasibility of our one-step β-Ga_2O_3 wafers for device fabrication, a simple metal–semiconductor–metal (MSM) structure photodetector was fabricated directly on the as-obtained β-Ga_2O_3 wafer. An interdigital electrode consisting of 10 nm titanium (Ti) and 40 nm gold (Au) was directly deposited on the β-Ga_2O_3 wafer using a shadow mask by thermal evaporation method. The electrode fingers were 200 μm wide with a 200 μm spacing gap. The schematic is shown in Fig. 8a. The time-dependent photo-response measurement was performed at a constant voltage of 10 V.

The spectral response is shown in Fig. 8b, indicating that the β-Ga_2O_3 MSM structure photodetector was sensitive to the solar-blind spectra range and possessed high spectral selectivity. The operation speed of the device was determined by performing time-resolved measurement, as shown in Fig. 8c and d. The time taken for the photocurrent to increase from 10% to 90% of the maximum photocurrent or *vice versa* was defined as the response time (t_r) and decay time (t_d), respectively. From the enlarged view, t_r and t_d were estimated to be 4.4 and 0.14 s, respectively, and it was expected that photoresponse times of the β-Ga_2O_3 MSM photodetector could be further improved *via* optimizing the device structure in future. The good

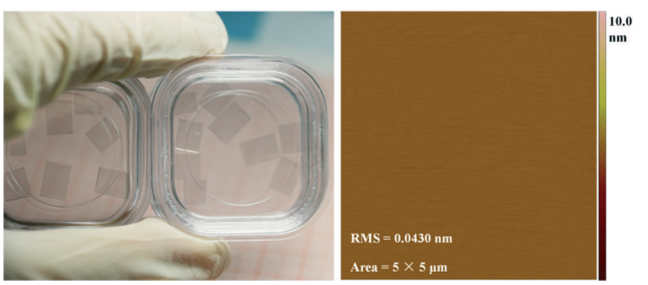

Fig. 7 Epi-ready wafers and AFM image of the exfoliated crystal wafer.

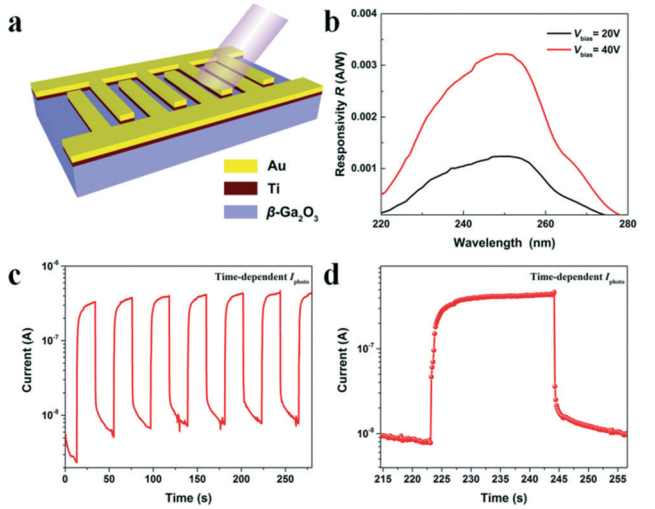

Fig. 8 (a) Schematic of the β-Ga_2O_3 single crystal MSM structure photodetector. (b) Spectroscopic responsivity of the β-Ga_2O_3 MSM structure photodetector. (c) Time response of the β-Ga_2O_3 MSM structure photodetector. (d) Enlarged view of the current rise and decay process.

performance of the device verified that the β-Ga_2O_3 wafer was feasible for application in devices. Furthermore, the wafers could also be used as substrates for homoepitaxy or heteroepitaxy, benefiting from the high quality of the surface. The epitaxy results on the exfoliated wafer will be reported later.

Conclusions and prospect

In this work, it was found that crystal cracking and polycrystals can be effectively prevented by using 1 inch-wide seeds. High-quality β-Ga_2O_3 single crystal with 25 mm width and 98 mm length was successfully grown by the optimized growth technique. Optical characterization showed that β-Ga_2O_3 exhibited a very broad transmission range from 0.26 to 7.33 μm. The bandgap of β-Ga_2O_3 was estimated to be 4.73 eV. Large-sized and high surface quality β-Ga_2O_3 wafers were obtained by the simple mechanical exfoliation method. This method has the advantages of being ultra-smooth, low-cost, one-step, no requirement of cutting, grinding and polishing for the wafer surface. The mechanism of the exfoliation method and effects of annealing process are analyzed from a crystallographic viewpoint. MSM structure photodetector based on the exfoliated wafer with fast response and decay time and high spectral selectivity has been demonstrated. All the results indicate that the exfoliated wafers are promising in semiconductor industry.

Conflicts of interest

There are no conflicts to declare.

Acknowledgements

This work has been supported by the National Natural Science Foundation of China (Grant No. 51321091, 51202128, 51227002 and 51323002), the Young Scholars Program of Shandong University (YSPSDU, 2015WLJH36), and National Key Research and Development Program of China (Grant No. 2016YFB1102201).

Notes and references

1 S. Fujita, *Jpn. J. Appl. Phys.*, 2015, **54**(3), 836–845.
2 E. Monroy, F. Omnès and F. Calle, *Semicond. Sci. Technol.*, 2003, **18**(4), R33–R51.
3 M. N. Yoder, *IEEE Trans. Electron Devices*, 1996, **43**(10), 1633–1636.
4 S. Pimputkar, J. S. Speck, S. P. DenBaars and S. Nakamura, *Nat. Photonics*, 2009, **3**(4), 180–182.
5 J. Millan, P. Godignon, X. Perpina, A. Perez-Tomas and J. Rebollo, *IEEE Trans. Power Electron.*, 2014, **29s**(5), 2155–2163.
6 H. Morkoç, S. Strite, G. B. Gao, M. E. Lin, B. Sverdlov and M. Burns, *J. Appl. Phys.*, 1994, **76**(3), 1363–1398.
7 C. Buttay, D. Planson, B. Allard, D. Bergogne, P. Bevilacqua, C. Joubert, M. Lazar, C. Martin, H. Morel, D. Tournier and C. Raynaud, *Mater. Sci. Eng., B*, 2011, **176**, 283.
8 Ü. Özgür, Y. I. Alivov, C. Liu, A. Teke, M. A. Reshchikov, S. Doğan, V. Avrutin, S.-J. Cho and H. Morkoç, *J. Appl. Phys.*, 2005, **98**, 041301.
9 M. Higashiwaki, K. Sasaki, A. Kuramata, T. Masui and S. Yamakoshi, *Appl. Phys. Lett.*, 2012, **100**, 013504.
10 M. Higashiwaki, K. Sasaki, T. Kamimura, M. Hoi Wong, D. Krishnamurthy, A. Kuramata, T. Masui and S. Yamakoshi, *Appl. Phys. Lett.*, 2013, **103**, 123511.
11 K. Sasaki, M. Higashiwaki, A. Kuramata, T. Masui and S. Yamakoshi, *J. Cryst. Growth*, 2013, **378**, 591–595.
12 W. S. Hwang, A. Verma, H. Peelaers and V. Protasenko, *Appl. Phys. Lett.*, 2014, **104**, 203111.
13 T. Oshima, T. Okuno and S. Fujita, *Jpn. J. Appl. Phys.*, 2007, **46**(11), 7217–7220.
14 R. Suzuki, S. Nakagomi and Y. Kokubun, *Appl. Phys. Lett.*, 2011, **98**, 131114.
15 D. Guo, Z. Wu, P. Li, Y. An, H. Liu, X. Guo, H. Yan, G. Wang, C. Sun, L. Li and W. Tang, *Opt. Mater. Express*, 2014, **4**, 1067–1076.
16 L. Mazeina, Y. N. Picard, S. I. Maximenko, F. K. Perkins, E. R. Glaser, M. E. Twigg, J. A. Freitas and S. M. Prokes, *Cryst. Growth Des.*, 2009, **9**(10), 4471–4479.
17 K. Shimamura, E. G. Víllora, K. Domen, K. Yui, K. Aoki and N. Ichinose, *Jpn. J. Appl. Phys.*, 2005, **44**, L7–L8.
18 S. Geller, *J. Chem. Phys.*, 1960, **33**, 676–684.
19 R. Roy, V. G. Hill and E. F. Osborn, *J. Am. Chem. Soc.*, 1952, **74**, 719–722.
20 A. O. Chase, *J. Am. Ceram. Soc.*, 1964, **47**, 470–470.
21 E. G. Víllora, K. Shimamura, Y. Yoshikawa, K. Aoki and N. Ichinose, *J. Cryst. Growth*, 2004, **270**, 420–426.
22 Z. Galazka, R. Uecker, K. Irmscher, M. Albrecht, D. Klimm, M. Pietsch, M. Brützam, R. Bertram, S. Ganschow and R. Fornari, *Cryst. Res. Technol.*, 2010, **45**, 1229–1236.
23 Z. Galazka, K. Irmscher, R. Uecker, R. Bertram, M. Pietsch, A. Kwasniewski, M. Naumann, T. Schulz, R. Schewski, D.

Klimm and M. Bickermann, *J. Cryst. Growth*, 2014, **404**, 184–191.

24 H. Aida, K. Nishiguchi, H. Takeda, N. Aota, K. Sunakawa and Y. Yaguchi, *Jpn. J. Appl. Phys.*, 2008, **47**(11), 8506–8509.

25 W. Mu, Y. Yin, Z. Jia, L. Wang, J. Sun, M. Wang, C. Tang, Q. Hu, Z. Gao, J. Zhang, N. Lin, S. Veronesi, Z. Wang, X. Zhao and X. Tao, *RSC Adv.*, 2017, **7**, 21815–21819.

26 W. Mu, Z. Jia, Y. Yin, Q. Hu, Y. Li, B. Wu, J. Zhang and X. Tao, *J. Alloys Compd.*, 2017, **714**, 453–458.

27 K. Hoshikawa, E. Ohba, T. Kobayashi, J. Yanagisawa, C. Miyagawa and Y. Nakamura, *J. Cryst. Growth*, 2016, **447**, 36–41.

28 Y. Kim, S. S. Cruz, K. Lee, B. O. Alawode, C. Choi, Y. Song, J. M. Johnson, C. Heidelberger, W. Kong, S. Choi, K. Qiao, I. Almansouri, E. A. Fitzgerald, J. Kong, A. M. Kolpak, J. Hwang and J. Kim, *Nature*, 2017, **544**, 340–343.

29 Y. Hernandez, V. Nicolosi, M. Lotya, F. M. Blighe, Z. Sun, S. De, I. T. McGovern, B. Holland, M. Byrne, Y. K. Gun'Ko, J. J. Boland, P. Niraj, G. Duesberg, S. Krishnamurthy, R. Goodhue, J. Hutchison, V. Scardaci, A. C. Ferrari and J. N. Coleman, *Nat. Nanotechnol.*, 2008, **3**, 563–568.

30 J. N. Coleman, M. Lotya, A. O'Neill, S. D. Bergin, P. J. King, U. Khan, K. Young, A. Gaucher, S. De, R. J. Smith, I. V. Shvets, S. K. Arora, G. Stanton, H.-Y. Kim, K. Lee, G. T. Kim, G. S. Duesberg, T. Hallam, J. J. Boland, J. J. Wang, J. F. Donegan, J. C. Grunlan, G. Moriarty, A. Shmeliov, R. J. Nicholls, J. M. Perkins, E. M. Grieveson, K. Theuwissen, D. W. McComb, P. D. Nellist and V. Nicolosi, *Science*, 2011, **331**, 568–571.

31 N. K. Mahenderkar, Q. Chen, Y.-C. Liu, A. R. Duchild, S. Hofheins, E. Chason and J. A. Switzer, *Science*, 2017, **355**, 1203–1206.